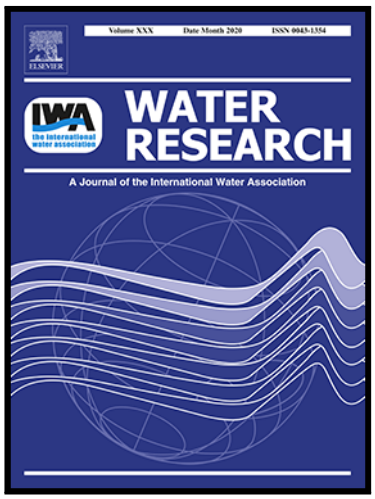

Effects of phytoplankton blooms on fluxes and emissions of greenhouse gases in a eutrophic lake

Maciej Bartosiewicz , Roxane Maranger , Anna Przytulska , Isabelle Laurion

PII: S0043-1354(21)00183-4
DOI: https://doi.org/10.1016/j.watres.2021.116985
Reference: WR 116985

To appear in: *Water Research*

Received date: 2 September 2020
Revised date: 24 February 2021
Accepted date: 25 February 2021

Please cite this article as: Maciej Bartosiewicz , Roxane Maranger , Anna Przytulska , Isabelle Laurion , Effects of phytoplankton blooms on fluxes and emissions of greenhouse gases in a eutrophic lake, *Water Research* (2021), doi: https://doi.org/10.1016/j.watres.2021.116985

8745 Words (including references), 4 tables and 6 figures

Effects of phytoplankton blooms on fluxes and emissions of greenhouse gases in a eutrophic lake

Maciej Bartosiewicz[1,2,3], Roxane Maranger[2,4], Anna Przytulska[1] and Isabelle Laurion[2,3]

[1]Department of Environmental Sciences, University of Basel, Basel, Switzerland.
[2]Groupe de recherche interuniversitaire en limnologie (GRIL).
[3]Centre Eau Terre Environnement, Institut national de la recherche scientifique, 490 de la Couronne, Québec, Canada.
[4]Département des Sciences Biologiques, Université de Montréal, C.P. 6128 succ. Centre-ville, Montréal, Canada.

Key words: global warming, phytoplankton blooms, carbon dioxide, methane, nitrous oxide, cyanobacteria, heatwaves, anoxia,

Research Highlights

- Heatwaves and cyanobacterial blooms influenced greenhouse gases in a lake.
- Anoxia associated to blooms and heatwaves enhanced CH_4 effluxes by up to 10 times.
- High CH_4 effluxes were associated with CO_2 and N_2O under-saturation at the surface.
- Cyanobacterial blooms stimulated CH_4 flux more than blooms of other phytoplankton.
- Synergy between blooms and heatwaves affects the role of lakes in the GHG budget.

Abstract (300 words)

Lakes are important sources of greenhouse gases (GHGs) to the atmosphere. Factors controlling CO_2, CH_4 and N_2O fluxes include eutrophication and warming, but the integrated influence of climate-warming-driven stratification, oxygen loss and resultant changes in bloom characteristics on GHGs are not well understood. Here we assessed the influence of contrasting meteorological conditions on stratification and phytoplankton bloom composition in a eutrophic lake, and tested for associated changes in GHGs inventories in both the shallow

and deep waters, over three seasons (2010-2012). Atmospheric heatwaves had one of the most dramatic effects on GHGs. Indeed, cyanobacterial blooms that developed in response to heatwave events in 2012 enhanced both sedimentary CH_4 concentrations (reaching up to 1mM) and emissions to the atmosphere (up to 8 mmol m^{-2} d^{-1}). That summer, CH_4 contributed 52% of the integrated warming potential of GHGs produced in the lake (in CO_2 equivalents) as compared to between 34 and 39% in years without cyanobacterial blooms. High CH_4 accumulation and subsequent emission in 2012 were preceded by CO_2 and N_2O consumption and under-saturation at the lake surface (uptakes at -30 mmol m^{-2} d^{-1} and -1.6 µmol m^{-2} d^{-1}, respectively). Fall overturn presented a large efflux of N_2O and CH_4, particularly from the littoral zone after the cyanobacterial bloom. We provide evidence that, despite cooling observed at depth during relatively hot summers, CH_4 emissions increased via stronger stratification due to surface warming, resulting in enhanced cyanobacterial biomass deposition and intensified bottom water anoxia. Our results, supported by recent literature reports, suggests a novel interplay between climate change effects on lake hydrodynamics that impacts both bloom characteristics and GHGs production in shallow eutrophic lakes. Given global trends of warming and enrichment, these interactive effects should be considered to more accurately predict the future global role of lakes in GHG emissions.

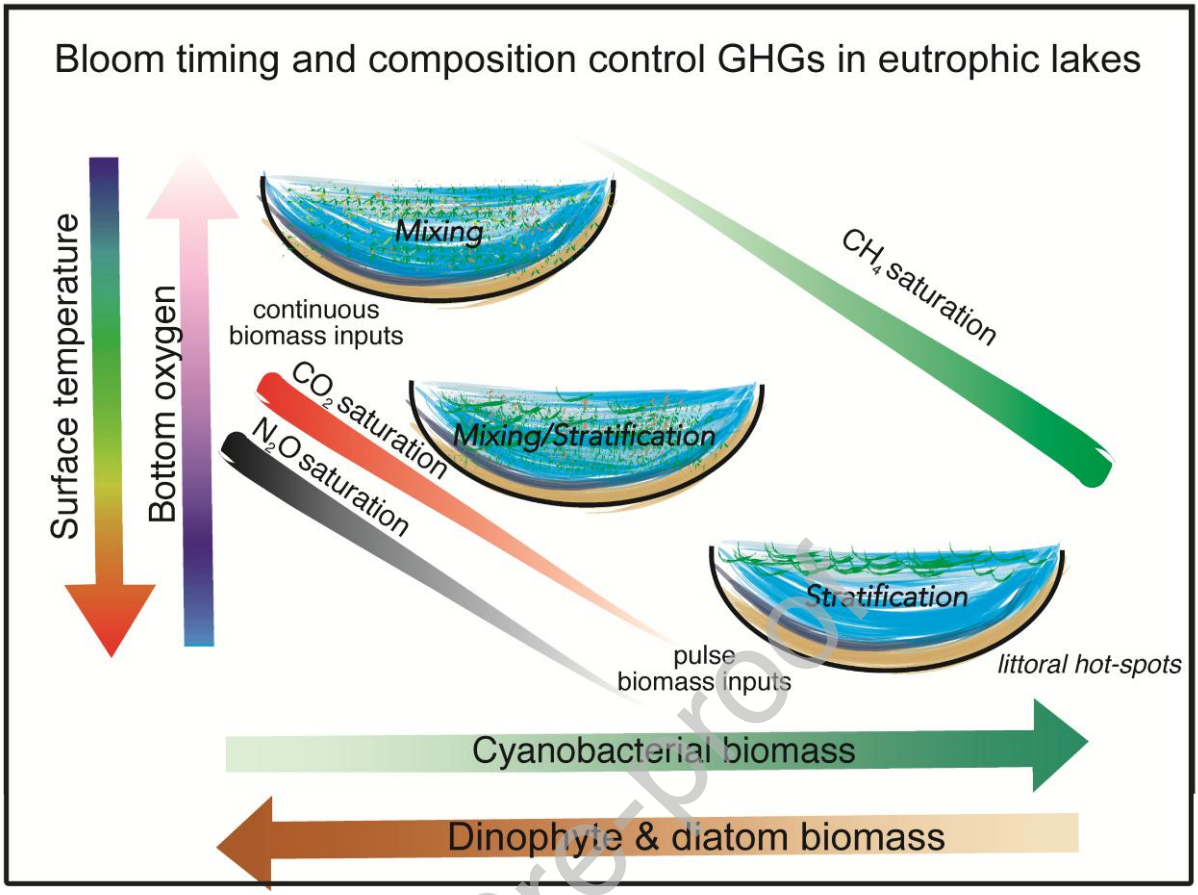

Introduction

Lakes emit relatively large amounts of greenhouse gases (GHG) to the atmosphere (Li et al., 2018). Contributions of CO_2, CH_4, and N_2O are influenced by temperature (Bartosiewicz et al., 2016), productivity (DelSontro et al., 2016), organic matter (OM) bio-lability (Grasset et al., 2018) and water column oxygenation (Vachon et al., 2019) among other factors. However, fluxes of these three gases are highly variable and often controlled by different drivers, influencing the warming potential of lakes (defined here by the cumulative emission in CO_2 equivalents considering the climate forcing potential of each gas). For example, while CO_2 supersaturation is prevalent in inland waters due to high inputs of terrestrial OM (Cole et al., 1994), lakes will, at times, also absorb atmospheric CO_2 when the photosynthetic consumption dominates over respiratory production (Grasset et al., 2020). Lakes can act as a source of N_2O to the atmosphere under eutrophic conditions (Xiao et al., 2018), but as a sink

when systems are hypereutrophic and strongly stratified (Webb et al., 2019). Broader scale geological and landcover features can cause lakes of an entire region to act as N_2O sinks under more oligotrophic conditions (Soued et al., 2016) as well as influence regional patterns in CO_2 saturation levels (Lapierre et al., 2017). Therefore, the combined relative strength of external forcing and within ecosystem responses can result in fluxes of varying strength and direction for these two GHGs.

While lakes are persistently oversaturated in CH_4, concentrations typically increase with increasing trophic status (DelSontro et al., 2018). Most of aqueous CH_4 is produced in anoxic sediments, and the fraction that avoids oxidation is released to the atmosphere through diffusion and ebullition. While oxidation was shown to reduce diffusive CH_4 fluxes by between 20 to 95% in temperate lakes depending on the lake depth, shape and stratification patterns (Bastviken et al., 2008), large CH_4 bubbles emerging almost exclusively from sediments are released directly to the atmosphere (DelSontro et al., 2016). Inputs of additional OM to sediments, be it through increased loading from the watershed or internal production, deplete the reservoir of oxidants and stimulate methanogenesis (Zhou et al., 2018), and as such, enhance evasion of CH_4 (Zhou et al., 2019). Although higher OM loads generally lead to higher benthic CH_4 production, the addition of fresh phytoplankton biomass is thought to stimulate methanogenesis more strongly as compared to terrestrial OM (Schwarz et al., 2008). Hence, conditions that favor increased phytoplankton biomass production and sedimentation should also favor CH_4 production, accumulation and emission. However, while the stimulation of methanogenesis by biomass additions under anoxia was shown experimentally (i.e., Grasset et al., 2019), the influence of in-situ phytoplankton community structure and emergence of noxious blooms on CH_4 flux, as well as on associated changes in CO_2 and N_2O fluxes, are still poorly understood.

As climate warms and lakes become more strongly stratified, internal nutrient loads can increase (Lau et al., 2020), stimulating the emergence of phytoplankton blooms (Woolway & Merchant, 2019) and enabling more persistent CO_2 depletion at the surface and oxygen shortages at the bottom (Bartosiewicz et al., 2019b). Proliferation of blooms in more strongly stratified waters can thus have major consequences for benthic OM processing (Yan et al., 2017) and planktonic food webs (Briland et al., 2020). For example, when the phytoplankton community is mainly composed of inedible biomass (i.e., filamentous cyanobacteria), a greater proportion of OM tends to reach the sediments after a bloom (Carey et al., 2012), strongly stimulating benthic respiration and methanogenesis. In fact, a positive relationship between the occurrence of toxic cyanobacterial blooms and CH_4 flux was recently reported from Lake Taihu in China (Yan et al., 2017). Furthermore, surface blooms themselves may enhance "thermal shielding" in the upper water column leading to bottom water cooling and prolonged anoxia, creating conditions that could respectively reduce OM processing and stimulate methanogenesis (Bartosiewicz et al., 2019b). Therefore, conditions that favor noxious blooms may also favor higher net CH_4 fluxes.

The combined effects of climate warming and eutrophication have stimulated cyanobacteria and other bloom forming phytoplankton in lakes worldwide (Huisman et al., 2018). Heatwave-associated thermal stratification tends to trigger these blooms and favor buoyant cyanobacteria (Jöhnk et al., 2008). As regional extreme heat events are increasing in frequency around the globe (Perkins-Kirkpatrick & Lewis, 2020) and phytoplankton blooms are becoming more severe (Gobler, 2020), their combined influence has possible cascading repercussions on GHGs. Here we used observational data collected in the pelagial and littoral zones of a nutrient-rich lake exposed to a spectrum of meteorological conditions, including heatwaves, to test the effects of hydrodynamic conditions on GHG storage and emissions. We specifically looked at how these conditions brought changes in the phytoplankton community

structure, bloom dynamics and water column oxygenation, and evaluated how these changes controlled the contribution of CO_2, CH_4 and N_2O to the cumulative warming potential of stored and released gases. This natural experiment by comparing three years allowed to test if buoyant cyanobacterial blooms influenced the efficiency of organic matter processing in the food web differentially than blooms by other phytoplankton, and assess the associated production, accumulation and efflux of GHGs in the pelagic and littoral zones of the lake.

Methods

Study site. Lake St. Augustin (46° 42'N, 71° 22'W, Fig. 1) is a small, shallow lake (0.62 km^2, max depth 6 m), classified as eutrophic to hypereutrophic (summertime TP = 20 - 160 $\mu g\ L^{-1}$ and Chl-a = 10 - 60 $\mu g\ L^{-1}$) located on the outskirts of Quebec City (Canada). During the past two centuries, this lake has been subjected to anthropogenic eutrophication (Deshpande et al., 2014) leading to persistent phytoplankton blooms from 1960 onward. Blooms in Lake Saint Augustin have been defined as periods when chl-a concentrations exceed 20 $\mu g\ L^{-1}$ and more than 80% of biomass is produced by one of the common bloom-forming species (i.e., *Glenodinium* sp or *Dolichospermum* sp.). The growing prevalence of cyanobacteria over the last two decades is in part due to an increase in water column stability and decrease in CO_2 availability under changing climate (Bartosiewicz et al., 2019a). Littoral and pelagial zones of the lake were defined based on the average light penetration depth estimated as two times the Secchi disk depth. In the littoral zones (< 2m deep), sunlight reached the bottom in spring allowing growth of the submerged macrophytes.

Physical chemistry and plankton dynamics. The lake was sampled during the open water season (from May to October) monthly in 2010 and 2011, and biweekly in 2012. During these

years, hourly air temperature, wind speed and precipitation data were obtained at the meteorological station of Environment Canada located 1.5 km from the lake (46°48'N, 71°23'W; http://climate.weather.gc.ca/). Vertical profiles of temperature, pH and dissolved oxygen (DO) were taken using a 600R multiparametric probe (Yellow Spring Instruments).

On each sampling date, discrete surface and near-bottom water samples taken at the deepest point of the lake were filtered through cellulose acetate filters (0.2-µm pore size) for the analyses of soluble reactive phosphorus (SRP, in duplicate, detection limit, DL = 0.5 µg L^{-1}) and nitrogen (N-NO^{3-}, DL = 0.01 mg L^{-1}) using standard colorimetric methods (Stainton et al., 1977). Total phosphorus and nitrogen were analyzed in a similar manner but on unfiltered water samples. Water collected at the surface of the littoral and pelagial sites (Fig. 2) was also filtered onto pre-combusted GF/F filters for the quantification of particulate OM. To determine the biovolume and composition of phytoplankton communities, 1 L water samples were collected at 1 m intervals from 0 to 5 m in the pelagial zone (littoral communities were not assessed). Subsamples from each depth were preserved with Lugol's iodine solution and analyzed following Utermöhl (1958) using an inverted microscope (Zeiss Axiovert 2000). For each phytoplankton species, at least 20 individuals were measured, and the biovolume was calculated following Hillebrand et al. (1999). Details on the phytoplankton community structure during the open-water season between 2010 and 2012 were presented by Bartosiewicz et al. (2019a).

Zooplankton were collected with a plankton net (63 µm) towed through the upper 3 m of the water column. Collected animals, preserved in formaldehyde, were identified according to Haney et al. (2013). The number of individuals counted per sample ranged from 150 to 600, and at least 20 individuals per identified species were measured and weighted biomass estimations (Gannon, 1971).

Greenhouse gas concentrations. A total of 950 GHG samples were collected between 2010 and 2012. Concentrations of dissolved CO_2, CH_4 and N_2O were collected by equilibrating 2 L of lake water with 20 mL of ambient air. After equilibration, the headspace was sampled into 6 mL He-purged, pre-evacuated Exetainers (Labco Limited, UK) for CO_2 and CH_4 analyses (triplicate samples), and the collected gas was analyzed with a gas chromatograph (Varian 3800) equipped with a methanizer and a flame ionization detector. Separate samples were taken for N_2O determination (also in triplicates): headspace samples were injected into 9 mL pre-evacuated borosilicate vials, and concentrations were determined with a gas chromatograph (Schimatzu 2014) equipped with an electron capture detector. During each sampling, 10ml of air was collected into 9ml for ambient atmospheric N_2O concentration measurements.

Aqueous gas concentrations were obtained using Henry's law and ambient water temperatures measured during the equilibration process. Global values of atmospheric partial pressures (400 ppm of CO_2 and 1.8 ppm of CH_4) were used to determine the CO_2 and CH_4 saturation levels, while local measurements of atmospheric partial pressures were used to determine N_2O saturation. To assess GHG storage in the lake, concentrations in the water column taken at 1 m resolution were multiplied by the volume of each respective depth interval and summed over the water column of both the littoral (0-2 m deep) and the pelagial zones (2-5m deep).

Greenhouse gas emissions. Diffusive flux at the air-water interface was estimated by multiplying the partial pressure of the gas with the piston velocity (k):

$$\text{Flux} = k \times \Delta\text{GHG}$$

where ΔGHG is departure from saturation for a given gas calculated as:

$$\Delta\text{GHG} = C_w - \alpha\, C_{air}$$

where C_w and C_{air} are the concentrations of gas respectively in water and air, and α is the Ostwald solubility coefficient; atmospheric gas is assumed dissolved at the top of the aqueous boundary layer. Piston velocity was calculated using the classic wind-based equation of Cole and Caraco (1998, hereafter CC) $k_{600} = 2.07 + 0.215 \times U^{1.7}$, where U is wind speed (m s^{-1}) at 10 meters height. We also used the wind-based equation corrected for lake size of Vachon and Prairie (2013, hereafter VP) $k_{600} = 2.51 + 1.48 \times U10 + 0.39 \times U \times log10\ LA$, where LA is the lake area (km^2). The *k* of individual gases was corrected using the Schmidt numbers (S_c) of CH_4, N_2O and CO_2 following the equation $k = k_{600}\ (S_c/600)^C$, where C equals -0.5 for rough surfaces and winds generally stronger than 3.5 m s^{-1} (Csanady, 1990). The CO_2 flux estimations were corrected for the chemical enhancement effects with the formula by Hoover and Berkshire (1969) using pH, wind speed and water temperature. Validation of the modeled GHG flux estimates was performed by comparison to direct CO_2 flux measurements done using a floating chamber in 2011 and 2012 (for details on chamber design and sampling scheme see Bartosiewicz et al., 2019a). Results from both the CC and VP models strongly correlated to measured chamber CO_2 fluxes (R^2=0.68 and 0.62, respectively, $p < 0.01$, $n = 24$). The VP model estimates better reflected the flux range obtained through direct measurements (slope closer to 1), and this model was henceforth retained for analyses in the following sections. Ebullition rates were determined (only in 2011 and 2012) by collecting gas bubbles with inverted PCV funnels coupled to a gas tight syringe in August 2011 (n = 6) and in June, July, August and September 2012 (n = 54) in both the littoral and pelagial zones of the lake.

Sediment profiling of CH_4. Porewater samples were collected in 2012 by in-situ dialysis at a 1-cm vertical sampling resolution 5 cm above and below the sediment interface using acrylic peepers. Before deployment, the peepers were conditioned under a N_2 atmosphere, with the gas renewed daily for two weeks to remove any traces of oxygen from the acrylic casting and

sampling wells. Sampling wells were filled with anoxic ultrapure water and covered with a polysulfone membrane (0.2-µm pore size, Gelman HT-200). Peepers (in triplicates) were transported in N_2-filled containers and placed in the lake for two to three weeks. Only porewater CH_4 concentration profiles were modeled assuming steady state conditions and neglecting the effect of advection and bioturbation (Clayer et al., 2020), with the general one-dimensional diagenetic transport-reaction equation for solutes:

$$\frac{\partial}{\partial x}\left(\varphi D_s \frac{\partial C}{\partial x}\right) + \varphi\alpha(C_{wat} - C) + R_{net}^{CH_4} = 0$$

where C and C_{wat} denote CH_4 concentrations respectively in porewater and in the burrows of benthic animals (assumed to be identical to that in sediment overlying water), x is the depth (positive downward), φ is the porosity, D_s is the effective diffusion coefficient, α is the bio-irrigation coefficient, and R_{net} is the net production rate (or consumption rate if R is negative) of CH_4 in a given sediment volume. The effective diffusion coefficient (Clayer et al., 2020) was calculated as:

$$D_s = \varphi^2 D_w$$

where D_w is the diffusion coefficient of CH_4 in water. The software PROFILE (Berg et al., 1998) was used to solve the equation for R, implementing average CH_4 concentration profiles (n = 3), measured φ values, and D_w values corrected for in situ temperature. The effective diffusion in and from the sediments was also calculated using PROFILE. The modelled and measured concentrations of CH_4 in the sediments were used to calculate the mass of this gas that accumulated in surface sediments by multiplying with respective volumes of porewater in the littoral and pelagial zones of the lake measured at 1 cm intervals.

Results

Surface meteorology. Air temperatures over Lake St. Augustin in 2010 and 2012 were on average warmer than in 2011 (Table 1), and well above the long-term normal (17.9°C between 1948 and 2010, Environment Canada 2012 Climate Report). The cooler summer of 2011 was also relatively wetter than those of 2010 and 2012. Weather in 2010 was also characterized by mild winter (4.0°C above normal, the warmest since 1948), followed by a warm spring (temperatures reaching 25°C in April; March to May average of 12.6°C, compared to 7.7°C in 2011). Average springtime temperature was also high in 2012 (11.1°C) and remained hot throughout the summer. One of the major differences among years was the relative exposure to heatwaves when air warmed beyond the pre-defined threshold of 31°C for at least 24h. Early in summer 2010, there were three heatwave days in June, whereas during the summer of 2012, the lake was exposed to four consecutive atmospheric heatwaves for a total of 11 days in July and early August. In 2011, there were no heatwaves recorded.

The lake warmed more at the surface in 2010 and 2012 as compared to 2011, with 2012 being the hottest on average (Table 1). Bottom waters, however, remained cooler in 2010 and 2012 (and coldest in 2012). Calm conditions during heat events strongly enhanced stratification (buoyancy frequency reaching 40 cph in surface waters) and heat losses were noticeably low on calm hot nights (i.e., 100 W m^{-2}). During these heatwaves, mixed layer deepening was suppressed, and the heat retained at the surface thermally shielded its bottom. The mechanistic explanation for the enhanced stratification upon warming in Lake St. Augustin was recently provided in Bartosiewicz et al. (2019b).

Oxygen conditions and nutrients. The bottom waters of the lake (3.5 to 5.5m) were better ventilated in summer 2011 as compared to 2010 and 2012 (Table 1, Figs. 2 & 3B), likely as a function of higher precipitation and strong nocturnal winds. The oxygen concentrations in the water directly overlaying sediments dropped below 0.2 mg L^{-1} (sensor detection limit) by late

July and early August in 2012, indicating that surface sediments likely became anoxic at that time. In contrast to bottom waters, surface oxygen concentrations were often well above saturation. The highest values were measured during the phytoplankton blooms occurring in August 2010 and July 2012 (reaching 150% of oxygen saturation). Differential stratification and oxygenation of the water column was reflected in differences between total and dissolved nutrient concentrations (TN, TP, N-NO_3^-, SRP). In fact, total nutrient concentrations were respectively higher and dissolved were lower in the warmer years as compared to the average year (except for N-NO_3^- in 2010), particularly when comparing 2012 with 2011.

Planktonic communities. During years with heatwaves (2010, 2012), cyanobacteria became more abundant in the lake as compared to the year without heatwaves (2011, Fig. 3A). In 2010, for example, an early biomass peak of buoyant filamentous cyanobacteria (*Aphanizomenon sp*.) occurred already in spring (June) accounting for as much as 72% of the total phytoplankton biomass (reaching 54 mg of wet weight L^{-1}). Following this peak, the phytoplankton community was dominated (up to 99%) by dinophytes that bloomed in mid-summer and by diatoms in fall (Fig. 3A). In 2012, we observed a massive occurrence of cyanobacteria that accumulated at the surface of the lake between mid-July and mid-August. High densities of *Aphanizomenon flos-aquae* and *Dolichospermum sp.,* reaching 47 × 10^3 cells mL^{-1} (up to 300 mg WW L^{-1}), were moved inshore by the wind later in the summer, where they likely settled to the bottom. By contrast, in 2011, the phytoplankton was dominated by diatoms in May (84% of 12 mg WW L^{-1}), followed by dinophytes (97% of the 98 mg WW L^{-1}) in June and July. Dinophytes together with diatoms formed an extensive bloom in the upper water column (up to 400 mg WW L^{-1}). The cumulative biomass of main phytoplankton groups (bloom forming diatoms, dinophytes and cyanobacteria) in the euphotic zone (taken throughout the studied periods as twice the Secchi depth) differed between years (one-way

ANOVA p=0.001, F=31.7) reaching up to 270 kg × 10^3 WW in 2010, up to 225 kg × 10^3 WW in 2011, and as much as 180 kg × 10^3 WW in 2012 (Fig. 3).

In 2012, the zooplankton biomass was higher than in 2011 on average (163 vs 116 µg DW L^{-1}; p = 0.02, t-test), but consisted of smaller species (e.g., *Ceriodaphnia* sp.). Large cladocerans (i.e., from the genus *Daphnia*), abundant in spring 2012, disappeared completely from the lake during the harmful cyanobacterial bloom (Fig. 3A). In 2011, by contrast, *Daphnia* were detected throughout the entire summer.

GHG concentrations. The CO_2 saturation level was variable between years and across the water column (Table 2), but remained persistently depleted during the hot and dry summer of 2012 (18.6 ± 15.5 µM, n=510) as compared to wet summer of 2011 (31.1 ± 17.9 µM, n=300), and the more intermediate summer of 2010 (43.7 ± 33.4 µM, n=140), with significant differences among years (one way-ANOVA, F=10.1, p=0.001). The mean CH_4 saturation level was higher in 2012 (0.59 ± 0.5 µM) than either in 2010 (0.50 ± 0.38 µM) or 2011 (0.46 ± 0.32 µM), but the interannual differences were not significant due to strong seasonality (p=0.3). N_2O was highest in 2012, but also extremely variable during that year (2.8 ± 4.2 nM). Spatially, there was less CO_2 at the surface of the littoral zone as compared to the pelagial zone (three-year average of 16.9 and 20.7 µM, respectively, t-test, p = 0.0001). In contrast, littoral surface waters were richer in CH_4 than those offshore (0.64 and 0.37 µM, p=0.001) and this was also true for N_2O (1.1 and 0.73 nM, p=0.001).

GHG emissions. CO_2 was released mostly through diffusion (>99%) with negligible fraction emitted through ebullition (<1%). The highly variable fluxes of CO_2 were, on average, lower in 2010 and 2012 (-7.1 ± 20.9 and -5.4 ± 29.7 mmol m^{-2} d^{-1}, respectively) than in 2011 (9.7 ± 26.1 mmol m^{-2} d^{-1}, Table 2). Thus, surface waters acted as a sink for atmospheric CO_2 in the

warmer summers (Fig. 4). The overturn period, subsequent to summertime blooms, resulted in large CO_2 emission to the atmosphere. In fact, the efflux during the 2012 overturn period was 30% higher than the maximum CO_2 efflux measured in 2011. In contrast to the pelagial zone, the littoral acted as a net CO_2 sink over this entire study (mean of -4.9 mmol m^{-2} d^{-1} inshore as compared to 5.5 mmol m^{-2} d^{-1} offshore for the 3 years merged, n=103, p=0.0001).

Diffusion was, on average, also the dominant pathway of CH_4 release from both littoral and pelagial zones (always >75%). Diffusive efflux from the pelagial zone was higher in 2012 (1.1 mmol m^{-2} d^{-2}, n = 61) than in 2010 (0.75 mmol m^{-2} d^{-1}, n = 12) or 2011 (0.85 mmol m^{-2} d^{-1}, n = 30), but given the large seasonal variability, this difference was not significant (ANOVA, p=0.09). The most striking difference among years was observed for the littoral zone, where the year with cyanobacterial blooms showed an average efflux that was twice as high (2.2 mmol m^{-2} d^{-1}) and significantly greater as over the two other years (1.1 mmol m^{-2} d^{-1} in 2010 and 0.9 mmol m^{-2} d^{-1} in 2011; p=0.001). Methane ebullition in 2011 (August only, n = 6) contributed about 1% (0.011 mmol m^{-2} d^{-1}) of the pelagial CH_4 efflux and about 17% (0.4 mmol m^{-2} d^{-1}) of the efflux from the littoral zone. For most of 2012, ebullition offshore was low (mean of 0.05 mmol m^{-2} d^{-1}; n=15) and contributed between 1 and 7% of the total CH_4 efflux. Only in relation to cyanobacterial blooms did the contribution of ebullition increase to 25%. Ebullition was much higher in the littoral zone (on average 0.53 mmol m^{-2} d^{-1}; n=15, p=0.001), contributing 11 to 75% of the CH_4 efflux (before and after the bloom, respectively). Ebullition was not measured in 2010.

The dominant emission pathways for N_2O was diffusion (>99%). Average N_2O flux from the pelagial zone of the lake was higher in 2011 (2.2 μmol m^{-2} d^{-1}) than in 2010 (0.53 μmol m^{-2} d^{-1}) or 2012 (0.91 μmol m^{-2} d^{-1}, $p<0.05$). Highest offshore N_2O emissions reached 8.6 μmol m^{-2} d^{-1} in September 2011. Overall, however, N_2O emissions were highest

from the littoral zone (2.0 μmol m^{-2} d^{-1} as compared to 1.4 μmol m^{-2} d^{-1} offshore; p=0.03, t-test).

Water column inventory of GHGs. Carbon dioxide was the dominant GHG accumulating in lake waters in 2010 and 2011, accounting for as much as 59% and 66% of the total ecosystem-scale efflux in CO_2 equivalents, respectively, with most of the remaining balance attributed to CH_4 (Fig. 3). In 2012 however, it was CH_4 that contributed most to the warming potential of the lake, averaging 52% of the ecosystem-scale efflux (in CO_2 eq.), with the contribution from dissolved CO_2 decreasing to 46%. The contribution from N_2O, albeit always small, increased to reach 2% of total emissions during the hot summer of 2012 (compared to less than 1% in 2010 and 2011) and was particularly high in the littoral zone.

The accumulation of GHGs in the water column of the littoral zone (<2 m deep) was proportional to its surface area (10% of the total lake area) in 2010 (i.e., up to 11% of CO_2 and CH_4, up to 5% of N_2O) and 2011 (up to 4% of CO_2 and up to 14% of CH_4). By comparison, shallow waters accumulated up to 20% of the total CH_4 and 18% of the total N_2O in 2012. The littoral zone contributed only about 6% of the warming potential of the lake over the three years of study despite the relatively high concentrations of CH_4 and N_2O measured there. This relatively low contribution by the littoral zone during the hot summer was caused by the persistent CO_2 depletion that occurred there.

Effects of cyanobacterial biomass on benthic CH_4. The CH_4 cumulating in surface sediments (down to 0.05 m, sampled only in 2012) increased by 2 to 5 times (in the littoral and pelagial sediments, respectively) after the cyanobacterial bloom collapsed in late August (Fig. 5). After the overturn period (September), the littoral sediments still stored considerable amounts of CH_4 (0.2×10^5 moles integrated over the entire zone) but mainly in the subsurface

(4-5 cm). On the other hand, the autumnal decrease of CH_4 observed in the offshore sediments implies that at this time, most of the accumulated gas in this section of the lake was already released or oxidized. The average CH_4 fluxes at the sediment-water interface were 20% higher after the cyanobacterial bloom than before it occurred (3.2 and 2.7 mmol m^{-2} d^{-1} in September and July, p=0.01, one-way ANOVA), and almost three times higher in the littoral than in the pelagial sediments (2.9 and 1.0 mmol m^{-2} d^{-1}).

Environmental controls on phytoplankton and relationship with GHGs. The biomass of dinophytes correlated to bottom and surface temperatures as well as to surface pH and O_2 levels but was inversely correlated to wind speeds and bottom O_2. The biomass of diatoms was correlated to wind speeds and bottom O_2 but was inversely correlated to surface temperatures. The cyanobacterial biomass was correlated to surface temperatures and inversely to bottom O_2 (Fig. 6; Table S1). The accumulation of CO_2 in the water column was correlated to bottom O_2 concentrations, to wind speeds and to diatom biomass (Fig. 6A), but inversely to surface O_2, pH, temperatures (surface and bottom), Chl-a and dinophyte biomass. CH_4 was positively correlated with water temperatures (bottom and surface), Chl-a and cyanobacterial biomass, and negatively with bottom O_2. N_2O correlated to water temperatures (surface and bottom).

The stepwise multiple regression analysis revealed that the combined effect of water temperatures and phytoplankton bloom composition explained a large fraction of the variability in GHGs accumulation (Fig 6; Table 3). Indeed, the stepwise regression model which included stratification strength (as the difference between surface and bottom water temperature) and biomass of non-cyanobacterial bloom formers (diatoms and dinophytes), explained 65% of the variability in water column CO_2 levels (p=0.0001); 54% of the variability in CH_4 accumulation was a function of surface water temperature and cyanobacterial biomass

(p=0.001), while changes in biomass of non-cyanobacterial bloom formers did not improve the regression; and finally, water temperature and stratification strength explained 43% of the variability in N_2O (p=0.005).

Discussion

Changes in phytoplankton bloom composition and timing influenced the warming potential of GHGs stored and released from Lake St. Augustin. Thermal shielding during hot years resulted in cooler bottoms, which likely diminished benthic processing through thermodynamic effects. However, the increase in CH_4 efflux observed after the heatwaves (i.e., enhanced by up to 10 times) resulted from the large inputs of cyanobacterial biomass to sediments. This higher deposition was also related to changes in the zooplankton community structure during the emergence of buoyant cyanobacteria, with small zooplankters being apparently unable to efficiently graze the accumulated biomass. In years with heatwaves, the lake was warmer at the surface and persistently more strongly stratified in 2012, which resulted in a faster and sustained depletion of oxygen at the lake bottom, as compared to 2011. These persistent low oxygen conditions set the stage for increased benthic CH_4 production enhanced due to freshly deposited biomass. In 2012, the biomass production was also associated to a sustained uptake of atmospheric CO_2 by buoyant cyanobacteria accumulating at the surface. These results imply that, under eutrophic conditions, the increased growth of buoyant filamentous cyanobacteria can stimulate benthic methanogenesis more than blooms of other phytoplankton (specifically, more edible dinophytes and diatoms) through direct pulse inputs of OM to anoxic sediments.

Effects of surface meteorology on phytoplankton blooms and consequences for GHGs

Phytoplankton phenology and community structure in Lake St. Augustin differed across studied years. Springtime warming in 2010 resulted in an early peak of cyanobacteria

followed by dinophytes and diatoms emerging when the lake was mixing relatively frequently during that summer. Wet and cool spring-to-summer transition in 2011, resulted in a community dominated by dinophytes with emergence of abundant diatoms later in the season. Hot and dry conditions in 2012 resulted in an early peak of dinophytes that were then replaced by cyanobacteria when the lake remained stratified for relatively long periods of time. Interannual differences in phytoplankton community structure and biomass patterns, despite sustained elevated nutrient concentrations among years (Table 1), suggest that eutrophication alone will not necessarily stimulate cyanobacterial blooms (Huang et al., 2020). Our observations in Lake St. Augustin suggest that it is the combined influence of eutrophication and stronger stratification as a function of warming that triggers cyanobacterial blooms in shallow eutrophic lakes which is expected to increase under the future climate (Bartosiewicz et al., 2019a).

Consequences of eutrophication were suggested to enhance the warming potential of gases emitted from temperate lakes through stimulated CH_4 and N_2O fluxes (DelSontro et al., 2018). Here we provide evidence that such effects are influenced by phytoplankton community structure as well as the timing and composition of seasonal blooms. Since cyanobacterial blooms are likely to proliferate as climate warms (Huisman et al., 2018), faster heat absorption within their buoyant biomass may stimulate stratification and reduce downward oxygen transport (Kumagai et al., 2000). The onset of anoxia favors OM processing towards CH_4 (Vachon et al., 2019) thus the carbon absorbed from the atmosphere by cyanobacteria (i.e., uptake of up to 30 mmol CO_2 m^{-2} d^{-1} in Lake St. Augustin) may later fuel methanogenesis at the bottom. This results from the inefficient processing (i.e., impaired grazing; see Bednarska & Dawidowicz, 2008) of filamentous cyanobacteria by zooplankton. In Lake St. Augustin, the large and efficient zooplankters (i.e., from the genus *Daphnia* sp.,) disappeared during and after the heatwaves when filamentous cyanobacteria became

abundant. It follows that, in the absence of grazing, cyanobacterial biomass was largely deposited to the sediments and increased benthic CH_4 fluxes and storage (Fig. 5).

While in many lakes CH_4 is known to be released mostly through ebullition (Aben et al., 2017; Zhou et al., 2019), the compact and clayed pelagial sediments in Lake St. Augustin apparently did not catalyze intense CH_4 bubbling. In fact, ebullition became important but only in association to cyanobacterial blooms (up to 25% of total CH_4 efflux in the pelagic zone). While our sampling design does not account for all possible point-source ebullition events (Wik et al., 2013), detection of higher ebullition rates (up to 75% of the total) in the organic-rich littoral sediments (OC > 20%), supports that CH_4 bubbling in this lake is controlled by sediment characteristics. Indeed, while warming catalyzed persistently high CH_4 efflux from shallow sediments, it was the combination of strong stratification and input of cyanobacterial biomass that triggered high CH_4 ebullition in the pelagial zone after the bloom had collapsed. The synergy between warming and eutrophication that may stimulate CH_4 ebullition (Aben et al. 2017; Davidson et al., 2018) appears as strongly variable in nature and, as implied by our observations, depends on the patterns of biomass re-distribution after blooms. These patterns will be particularly critical for buoyant biomass of filamentous bloom-formers that is often moved inshore by winds and deposited to sediments in the littoral zone.

Warming was also shown to influence activation energies during OM degradation and enhance the proportion of primary production released as CH_4 (Durocher et al. 2011; 2014). However, and counterintuitively, bottom waters (and offshore sediments) of Lake St. Augustin remained relatively cold during summer with heatwaves. The enhanced water column stratification leading to this cooling (Bartosiewicz et al. 2019b) was also conductive to CO_2 depletion at the surface and expansion of anoxia at the bottom. Arguably the exact outcome of such opposing effects on net CH_4 efflux, where bottom cooling slows down OM processing on the one hand and higher OM inputs enhance benthic methanogenesis on the other, will vary

with lake morphometry and food web structure. Our study, however, provides a first line of support for the importance of phytoplankton bloom composition as a driver of CH_4 production, with cyanobacterial dominance increasing its contribution to the overall warming potential of GHGs produced and emitted by a shallow lake ecosystem.

Spatiotemporally variable effects of phytoplankton blooms on GHGs

Ecosystem scale effects of heatwaves in 2012 generated about 28×10^3 moles CO_2 equivalent as compared to 31×10^3 moles CO_2 equivalent in 2011. This relatively small difference results mostly from the negative contribution of CO_2 up-taken by buoyant cyanobacteria in 2012. Despite high uptake rates at the surface, CO_2 still remained important GHG stored and released from the water column during both years. However, while the massive dinophyte bloom was not conducive to persistent CO_2 depletion in 2011, the combination of strong stratification and emergent buoyant cyanobacteria of 2012 lead to a persistent CO_2 undersaturation throughout the upper waters. This was not simply an effect of scale as the dinophyte bloom in 2011 lasted longer and produced higher biomass than the cyanobacterial bloom in the following summer. Noticeably, shallow littoral zones of the lake represented larger and mostly continuous sink for CO_2 as compared to the less consistent uptake in the pelagial zones. This may have resulted from the wind-driven concentration of buoyant cyanobacteria in the nearshore areas and from sustained CO_2 consumption by submerged macrophytes (i.e., *Myriophyllum* sp.; *Vallisneria americana*).

In support of our initial idea, when CO_2 was depleted, CH_4 became the most important GHG (in terms of CO_2 eq.) during summer with heatwaves and after the collapse of cyanobacterial blooms. However, while pelagial CH_4 flux increased by only ~20%, littoral emissions did so by ~50%. This raises the need to closely consider the spatiotemporal nature of phytoplankton productivity effects on GHGs emissions in lakes. Observed differences between pelagial and littoral zones may have emerged through stimulation of specific methanogens in near-shore sediments or from the relatively stronger vertical mixing in the shallows that limited the time-window available for methane oxidation (Mayr et al., 2020). The globally increasing frequency of heatwaves (Perkins-Kirkpatrick and Lewis, 2020) will

influence hydrodynamics differently in deep and shallow waters. Periods of intense warming and water column stabilization will apparently enhance rates of atmospheric CO_2 uptake but can also strongly stimulate CH_4 and N_2O emissions in the shallows. To improve future predictions and upscaled calculations, particular attention should be paid on where and what type of biomass is processed to GHGs during and after phytoplankton blooms. Lake morphometry thus becomes an important characteristic to factor in when estimating emissions at the scale of a lake.

Rates of CH_4 release from the pelagial sediments were lower than diffusion at the water surface in early summer 2012 (i.e., 0.5 mmol m^{-2} d^{-1} as compared to 1.8 mmol m^{-2} d^{-1}). This difference may be indicative of CH_4 production within the well-oxygenated upper water column (DelSontro et al., 2018) or, alternatively, transport of CH_4-rich waters from the littoral zone (Encinas-Fernández et al., 2016). The difference between benthic and surface CH_4 effluxes later in summer (2.6 mmol m^{-2} d^{-1} compared to 1.3 mmol m^{-2} d^{-1}, respectively) suggests that CH_4 oxidation was responsible for removal of about 50% of CH_4 from the pelagial zone, and 40% from the littoral zone. Sediment profiles reveal surficial decreases in CH_4 concentrations, particularly important in the littoral sediments (Fig. 5, lower panels). This may indicate zone of anaerobic CH_4 oxidation in surface sediments (Martinez-Cruz et al. 2018). Noticeably, the CH_4 concentrations decreased by 90 to 95% (from 3 to 1 cm below the sediment surface) in the pelagial and littoral zone, respectively. The efficiency of this CH_4 consumption was reduced after the cyanobacterial bloom collapsed, as CH_4 concentrations decreased respectively only by 45 to 72%. Speculatively, this may indicate a reduction in rates of anaerobic methanotrophy under OM-enriched conditions when fermenting bacteria become relatively more active (Yang et al., 2018).

Our study reveals large interannual, seasonal and spatial variability in N_2O concentrations and fluxes. In contrast to CH_4 and despite relatively large amounts of N_2O accumulated over the hot summer 2012 (Table 1), the mean efflux of this potent GHG was

higher during the rainy year (2011). Indeed, the largest N_2O release was observed in the littoral zone following strong autumnal rainfall, suggesting the potentially important role of allochthonous inputs and/or water intrusions in the production and release of N_2O. While the overall contribution from N_2O (in CO_2 eq.) can be considered negligible in this lake, its production was strongly enhanced in the shallow zones, and correlated to the deposition of bloom biomass on littoral sediments. While CH_4 and CO_2 fluxes appeared as coupled, with CH_4 increasing and CO_2 decreasing respectively during and after each phytoplankton bloom event, N_2O fluxes were rather decoupled from these other GHGs and related to allochthonous processes (i.e., rainfall in the catchment, Fig. 6B). Interestingly, during winter 2011 and 2012 (data not shown), we have recorded peaks in N_2O concentrations, with integrated mass reaching twice as much as during the summertime maximum. Such wintertime accumulation with potentially rapid release upon ice breakups has also been reported from multiple boreal lakes in Canada (Soued et al., 2016). This indicates the need for better resolved studies on N_2O dynamic in aquatic systems, aiming to identify hot emission moments of this potent GHG that can be apparently distinct from those reported for CH_4 and CO_2.

There has been an exponential increase in the number of studies reporting GHG emission rates from lakes over the last two decades (see selected recent work in Table 4). This rapidly growing literature unequivocally supports that lakes are important sources of CO_2, CH_4 and N_2O to the atmosphere, and that both warming and eutrophication strongly influence fluxes of these gases from sediments and throughout the water column. Most recent work has focused on determining environmental controls on CH_4 and N_2O, the two more potent GHGs, rather than on CO_2. A number of field, experimental, and modelling efforts established further that warming enhances CH_4 flux more strongly than CO_2 flux, likely as a consequence of more favorable conditions for methanogens arising under warmer ambient temperature (Table 4). When assessed in combination, eutrophication and warming was suggested to act synergistically to change the magnitude of GHGs effluxes from lakes (Table 4). In light of this literature survey and our own work, we argue that understanding the effects

of phytoplankton bloom characteristics and resulting food web changes, directly controlled by eutrophication and warming, is needed to fully appreciate and predict GHG fluxes in freshwaters. Our work provides the first comprehensive assessment of how phytoplankton bloom composition and phenology, influenced by local climate and eutrophication, affects GHGs. Furthermore, the novel mechanism of enhanced CH_4 production mediated through the sedimentation of cyanobacterial bloom potentially represents a positive climate-cyanobacteria-methane feedback that has important implications for future predictions on global GHGs budget. Indeed, if warming and eutrophication lead to further proliferation of cyanobacterial blooms in lakes, proportionally higher CH_4 production (even if from recently fixed CO_2) may lead to an accelerated atmospheric warming through enhanced emissions from lakes.

Conclusions

Spatiotemporal variability in GHG production, accumulation and release from a small, nutrient-rich lake was shown to depend on the type and phenology of phytoplankton blooms. Our results suggest that proliferation of buoyant filamentous blooms, stimulated by warming and water column stability, can result in enhanced CH_4 production and fluxes at the expense of CO_2. If correct, the positive feedback effect between the formation of cyanobacterial blooms and climate change will include reciprocal stimulation between these two processes. We also evidence that, despite the cooling occurring at depth, benthic CH_4 emissions increased through a synergy between anoxia and higher pulse biomass deposition. This effect boosted CH_4 fluxes both at the sediment-water and at the water-atmosphere interfaces. Effects of eutrophication and higher production on CH_4 flux are not, however, necessarily linear as increasing biomass produced under nutrient-rich conditions can be processed efficiently to CO_2 through trophic transfer and respiration (such as for Lake St. Augustin in 2011). For future climate projections, it will be important to consider the emerging synergies between

effects of warming on water temperatures, stratification strength and oxygenation, bloom phenology and composition, as well as patterns of carbon transfer in the food web. Understanding interactive effects between phytoplankton production and consumption, as well as planktonic OM redistribution into different carbon pools (including CH_4) from sediments into the overlaying waters, appears crucial to accurately predict the role of lakes in the global GHGs budget under future climate and eutrophication scenarios.

Declaration of interests

☒ The authors declare that they have no known competing financial interests or personal relationships that could have appeared to influence the work reported in this paper.

☐The authors declare the following financial interests/personal relationships which may be considered as potential competing interests:

References

Aben, R.C.H., Barros, N., van Donk, E., T. Frenken, T., Hilt, S., Kazanjian, G., L.P.M. Lamers, L.P.M., E. Peeters, E., Roelofs, J.G.M., L.N. de Senerpont Domis, L.N., Stephan, S., M. Velthuis, Van de Waal, D.B., Wik, M., Thornton, B.F., Wilkinson, J., DelSontro, T., Kosten, S., 2017. Cross continental increase in methane ebullition under climate change. Nature Communications 8 (1), 1682.

Audet, J., Neif, É. M., Cao, Y., Hoffmann, C. C., Lauridsen, T. L., Larsen, S. E., Davidson, T. A., 2017. Heat-wave effects on greenhouse gas emissions from shallow lake mesocosms. Freshwater Biology 62(7), 1130–1142.

Bartosiewicz, M., Laurion, I., Clayer, F., Maranger, R., 2016. Heat-wave effects on oxygen, nutrients, and phytoplankton can alter global warming potential of gases emitted from a small shallow lake Environmental Science and Technology 50 (12), 6267–6275.

Bartosiewicz, M., Przytulska, A., Deshpande, B.N., Antoniades, D., Cortes, A., MacIntyre, S., Lehmann, M.F., Laurion, I., 2019a Effects of climate change and episodic heat events on

cyanobacteria in a eutrophic polymictic lake. Science of The Total Environment 693, 133414.

Bartosiewicz, M., Przytulska, A., Lapierre, J.F., Laurion, I., Lehmann, M.F., Maranger, R., 2019b. Hot tops, cold bottoms: synergistic climate warming and shielding effects in-crease carbon burial in lakes. Limnology and Oceanography Letters 4, 132–144.

Bastviken, D., Cole, J.J., Pace, M.L., Van de Bogert, M.C., 2008. Fates of methane from different lake habitats: connecting whole-lake budgets and CH_4 emissions. Journal of Geophysical Research Biogeosciences, 113, (G2) (2008) (2005–2012).

Beaulieu, J.J., DelSontro, T., Downing, J.A., 2019. Eutrophication will increase methane emissions from lakes and impoundments during the 21st century. Nature Communications 10, 1375.

Bednarska, A., Dawidowicz, P., 2007. Change in filter-screen morphology and depth selection: uncoupled responses of *Daphnia* to the presence of filamentous cyanobacteria. Limnology and Oceanography 52, 2358–2363.

Berg, P., Risgaard-Petersen, N., Rysgaard, S., 1998 Interpretation of measured concentration profiles in sediment pore water. Limnology and Oceanography 43, 1500–1510.

Briland, R.D., Stone, J.P., Manubolu, M., Lee, J., Ludsin, S.A., 2019. Cyanobacterial blooms modify food web structure and interactions in western Lake Erie. Harmful Algae 92, 101586.

Carey, C.C., 2012. The ecosystem effects of cyanobacteria in an oligotrophic lake. Dissertation. Cornell University, Ithaca, New York, USA.

Cheng, J., Xu, L., Jiang, M., Jiang, J., & Xu, Y., 2020. Warming Increases Nitrous Oxide Emission from the Littoral Zone of Lake Poyang, China. Sustainability, 12(14), 5674.

Clayer, F., Gélinas, Y., Tessier, A., Gobeil, C., 2020 Mineralization of organic matter in boreal lake sediments: Rates, pathways and nature of the fermenting substrates. Biogeosciences 17, 4571–4589.

Cole, J.J., Caraco, N.F., Kling, G.W., Kratz, T.K., 1994. Carbon dioxide supersaturation in the surface waters of lakes. Science 265, 1568–1570.

Cole, J.J., Caraco, N.F., 1998. Atmospheric exchange of carbon dioxide in a low-wind oligotrophic lake measured by the addition of SF_6. Limnology and Oceanography 43, 647–656.

Csanady, G. T., 1990. The role of breaking wavelets in air-sea gas transfer. Journal of Geophysical Research: Oceans, 95(C1), 749–759.

Davidson, T. A., Audet, J., Svenning, J. C., Lauridsen, T. L., Søndergaard, M., Landkildehus, F., Jeppesen, E., 2015. Eutrophication effects on greenhouse gas fluxes from shallow-lake mesocosms override those of climate warming. Global Change Biology, 21(12), 4449–4463.

Davidson, T.A., Audet, J., Jeppesen, E., Landkildehus, F., Lauridsen, T.L, Søndergaard, M., Syväranta, J., 2018. Synergy between nutrients and warming enhances methane ebullition from experimental lakes. Nature Climate Change 8, 156–160.

DelSontro, T., Boutet, L., St-Pierre, A., Del Giorgio, P.A., Prairie, Y.T., 2016. Methane ebullition and diffusion from northern ponds and lakes regulated by the interaction between temperature and system productivity. Limnology and Oceanography 61, 62–77.

DelSontro, T., Beaulieu, J.J., Downing, J.A., 2018. Greenhouse gas emissions from lakes and impoundments: upscaling in the face of global change. Limnology and Oceanography Letters 3, 64–75.

Deshpande, B.N., Tremblay, R., Pienitz, R., Vincent, W.F., 2014. Sedimentary pigments as indicators of cyanobacterial dynamics in a hypereutrophic lake. Journal of Paleolimnology 52, 171–184.

Devlin, S. P., Saarenheimo, J., Syväranta, J., Jones, R. I., 2015. Top consumer abundance influences lake methane efflux. Nature Communications 6, 8787.

Encinas Fernández, J., Peeters, F., Hofmann, H., 2016. On the methane paradox: transport from shallow water zones rather than in situ methanogenesis is the major source of CH_4 in the open surface water of lakes. Journal of Geophysical Research Biogeosciences 121, 2717–2726.

Fernandez, J. M., Townsend-Small, A., Zastepa, A., Watson, S. B., Brandes, J. A., 2020. Methane and nitrous oxide measured throughout Lake Erie over all seasons indicate highest emissions from the eutrophic Western Basin. Journal of Great Lakes Research 46(6), 1604–1614.

Gannon, J.E., 1971. Two counting cells for the enumeration of zooplankton micro-Crustacea. Transactions of the American Microscopical Society, 90, 486–490.

Gobler, C.J., 2020. Climate change and harmful algal blooms: insights and perspective. Harmful Algae, 91, 101731.

Gonzalez-Valencia, R., Sepulveda-Jauregui, A., Martinez-Cruz, K., Hoyos-Santillan, J., Dendooven, L., Thalasso, F., 2014. Methane emissions from Mexican freshwater bodies: correlations with water pollution. Hydrobiologia 721(1), 9–22.

Grasset, C., Mendonca, R., Saucedo, G.V., Bastviken, D., Roland, F., Sobek, S., 2018. Large but variable methane production in anoxic freshwater sediment upon addition of allochthonous and autochthonous organic matter. Limnology and Oceanography 63, 1488–1501.

Grasset, C., Abril, G., Mendonça, R., Roland, F., Sobek, S., 2019. The transformation of macrophyte-derived organic matter to methane relates to plant water and nutrient contents. Limnology and Oceanography 64(4), 1737–1749.

Grasset C., Sobek S., Scharnweber K., Moras S., Villwock H., Andersson S., Tranvik J. L., 2020. The CO_2-equivalent balance of freshwater ecosystems is non-linearly related to productivity. Global Change Biology 26, 5705– 5715.

Haney J.F., et al. 2013. "An-Image- based Key to the Zooplankton of North America" version 5.0. http://cfb.unh.edu/cfbkey/html/

Hillebrand, H., Dürselen, C.D., Kirschtel, D., Pollingher, U., Zohary, T., 1999. Biovolume calculation for pelagic and benthic microalgae. Journal of Phycology 35, 403–424.

Huisman, J., Codd, G.A., Paerl, H.W., Ibelings, B.W., Verspagen, J.M.H., Visser, P.M., 2018. Cyanobacterial blooms. Nature Reviews Microbiology 16 (8), 471–483.

Jöhnk, K.D., Huisman, J.E.F., Sharples, J., Sommeijer, B.E.N., Visser, P.M., Stroom, J.M., 2008. Summer heatwaves promote blooms of harmful cyanobacteria. Global Change Biology 14, 495–512.

Klaus, M., Bergström, A. K., Jonsson, A., Deininger, A., Geibrink, E., & Karlsson, J., 2018. Weak response of greenhouse gas emissions to whole lake N enrichment. Limnology and Oceanography, 63(S1), 340–353.

Kumagai, M., Nakano, S., Jiao, C., Hayakawa, K., Tsujimura, S., Nakajima, T., Frenette, J., Quesada, A., 2000. Effect of cyanobacterial blooms on thermal stratification. Limnology, 1, 191–195.

Lapierre, J.F., Seekell, D., Filstrup, C.T., Collins, S.M., Fergus, C. E., Soranno, P.A., Cheruvelil, K.S., 2017. Continental-scale variation in controls of summer CO_2 in United States lakes. Journal of Geophysical Research Biogeosciences 122(4), 875–885.

Lau, M. P., Valerio, G., Pilotti, M., Hupfer, M., 2020. Intermittent meromixis controls the trophic state of warming deep lakes. Scientific Reports 10(1), 1–16.

Li, S., Bush, R.T., Santos, I.R., Zhang, Q., Song, K., Mao, R., Wen, Z., Lu, X.X., 2018. Large greenhouse gases emissions from China's lakes and reservoirs. Water Research 147, 13–24.

Li, M., Peng, C., Zhu, Q., Zhou, X., Yang, G., Song, X., Zhang, K., 2020. The significant contribution of lake depth in regulating global lake diffusive methane emissions. Water Research 172, 115465.

Martinez-Cruz, K., Sepulveda-Jauregui, A., Casper, P., Anthony, K.W., Smemo, K.A., Thalasso, F., 2018. Ubiquitous and significant anaerobic oxidation of methane in freshwater lake sediments. Water Research 144,332–340.

Mayr, M.J., Zimmermann, M., Guggenheim, C., Brand, A., Buergmann, H., 2020. Niche partitioning of methane-oxidizing bacteria along the oxygen-methane counter gradient of stratified lakes. ISME Journal 14 (1), 274–287.

Pacheco, F. S., Roland, F., & Downing, J. A., 2014. Eutrophication reverses whole-lake carbon budgets. Inland Waters 4(1), 41–48.

Perkins-Kirkpatrick S.E., Lewis S.C., 2020. Increasing trends in regional heatwaves. Nature Communications 11(1), 1–8.

Pu, J., Li, J., Zhang, T., Martin, J. B., Yuan, D., 2020. Varying thermal structure controls the dynamics of CO2 emissions from a subtropical reservoir, south China. Water Research, 115831.

Salk, K. R., Ostrom, P. H., Biddanda, B. A., Weinke, A. D., Kendall, S. T., Ostrom, N. E., 2016. Ecosystem metabolism and greenhouse gas production in a mesotrophic northern temperate lake experiencing seasonal hypoxia. Biogeochemistry, 131(3), 303–319.

Schwarz, J.I., Eckert, W., Conrad, R., 2008. Response of the methanogenic microbial community of a profundal lake sediment (Lake Kinneret, Israel) to algal deposition Limnology and Oceanography 53, 113–122.

Soued, C., del Giorgio, P.A., Maranger, R., 2016. Nitrous oxide sinks and emissions in boreal aquatic networks in Québec. Nature Geoscience 9, 1–7.

Vachon, D., Prairie, Y.T., 2013. The ecosystem size and shape dependence of gas transfer velocity versus wind speed relationships in lakes. Canadian Journal of Fisheries and Aquatic Science 70 (12), 1757–1764.

Vachon, D., Langenegger, T., Donis, D., McGinnis, D.F., 2019. Influence of water column stratification and mixing patterns on the fate of methane produced in deep sediments of a small eutrophic lake. Limnology and Oceanography 64(5), 2114–2128.

Vachon, D., Langenegger, T., Donis, D., Beaubien, S. E., & McGinnis, D. F. (2020). Methane emission offsets carbon dioxide uptake in a small productive lake. Limnology and Oceanography Letters, 5(6), 384–392.

Wang, H., Lu, J., Wang, W., Yang, L., & Yin, C., 2006. Methane fluxes from the littoral zone of hypereutrophic Taihu Lake, China. Journal of Geophysical Research: Atmospheres, 111(D17).

Webb, J.R., Hayes, N.M., Simpson, G.L., Leavitt., P.R., Baulch, H.M., Finlay, K. 2019. Widespread nitrous oxide under-saturation in farm waterbodies creates an unexpected greenhouse gas sink. Proceedings of the National Academy of Sciences 116, 9814–9819.

West, W.E., Coloso J.J., Jones, S.E., 2012. Effects of algal and terrestrial carbon on methane production rates and methanogen community structure in a temperate lake sediment. Freshwater Biology 57 (5), 949–955.

West, W. E., Creamer, K. P., & Jones, S. E., 2015. Productivity and depth regulate lake contributions to atmospheric methane. Limnology and Oceanography 61(1), 51–61.

Wik, M., Crill, P.M., Varner, R.K., Bastviken, D., 2013. Multiyear measurements of ebullitive methane flux from three subarctic lakes, Journal of Geophysical Research Biogeosciences 118 (3), 1307-1321.

Woolway, R.I., Merchant, C.J., 2019. Worldwide alteration of lake mixing regimes in response to climate change. Nature Geoscience 12, 271–276.

Xiao, Q., Zhang, M., Hu, Z., Gao, Y., Hu, C., Liu, C., Lee, X. 2017. Spatial variations of methane emission in a large shallow eutrophic lake in subtropical climate. Journal of Geophysical Research: Biogeosciences, 122(7), 1597–1614.

Xiao, Q., Xu, X., Zhang, M., Duan, H., Hu, Z., Wang, W & Lee, X., 2019. Coregulation of nitrous oxide emissions by nitrogen and temperature in China's third largest freshwater lake (Lake Taihu). Limnology and Oceanography, 64(3), 1070–1086.

Yan, X.C., Xu, X.G., Wang, M.Y., Wang, G.X., Wu, S.J., Li, Z.C., 2017. Climate warming and cyanobacteria blooms: looks at their relationships from a new perspective, Water Research 125, 449–457.

Yang, Y.Y., Chen, J.F., Tong, T.L., Li, B.Q., He, T., Liu, Y., Xie, S.G., 2019. Eutrophication influences methanotrophic activity, abundance and community structure in freshwater lakes. Science of The Total Environment 662, 863–872.

Yvon-Durocher, G., Montoya, J.M., Trimmer, M., Woodward, G., 2011. Warming alters the size spectrum and shifts the distribution of biomass in freshwater ecosystems. Global Change Biology 17, 1681–1694.

Yvon- Durocher, G., Allen, A.P., Bastviken, D., Conrad, R., Gudasz, C., St-Pierre, A., Thanh-Duc, N., del Giorgio, P.A., 2014. Methane fluxes show consistent temperature dependence across microbial to ecosystem scales. Nature 507, 488–491.

Zhang, L., Liao, Q., Gao, R., Luo, R., Liu, C., Zhong, J., Wang, Z., 2020. Spatial variations in diffusive methane fluxes and the role of eutrophication in a subtropical shallow lake. Science of The Total Environment, 143495.

Zhang, L., Liu, C., He, K., Shen, Q., Zhong, J., 2020. Dramatic temporal variations in methane levels in black bloom prone areas of a shallow eutrophic lake. Science of The Total Environment, 144868.

Zhou, Y., Xiao, Q., Yao, X., Zhang, Y., Zhang, M., Shi, K., Jeppesen, E., 2018. Accumulation of terrestrial dissolved organic matter potentially enhances dissolved methane levels in eutrophic Lake Taihu, China. Environmental Science & Technology, 52(18), 10297–10306.

Zhou, Y.Q., Zhou, L., Zhang, Y.L., de Souza, J.G., Podgorski, D.C., Spencer, R.G.M., Jeppesen, E., Davidson, T.A., 2019. Autochthonous dissolved organic matter potentially fuels methane ebullition from experimental lakes. Water Research 166, 115048.

Zhou, Y., Song, K., Han, R., Riya, S., Xu, X., Yeerken, S., Terada, A., 2020. Nonlinear response of methane release to increased trophic state levels coupled with microbial processes in shallow lakes. Environmental Pollution, 114919.

Zhu, L., Qin, B., Zhou, J., Van Dam, B., & Shi, W., 2018. Effects of turbulence on carbon emission in shallow lakes. Journal of Environmental Sciences 69, 166–172.

Table 1. Surface meteorology (mean wind speed, rainfall and air/water temperature), as well as average dissolved oxygen saturation levels, total and dissolved nutrients (total phosphorus = TP, total nitrogen = TN, soluble reactive phosphorus = SRP; nitrate = NO_3) and productivity indices (total suspended solids = TSS, chlorophyll-a = Chl-a) between June and September on the three sampled years. n.d. – no data.

Variable	2010	2011	2012
Wind speed (m s^{-1})	3.3	3.5	3.0
Rain (mm)	340	410	230
Air Temperature (°C)	19.3	18.6	19.7
Surface temperature (°C)	22.6	21.4	24.1

Bottom temperature (°C)	18.2	18.5	17.6
Bottom oxygenation (%)	60	67	54
TP (μg L^{-1})	58	48	66
TN (μg L^{-1})	390	340	440
SRP (μg L^{-1})	2.5	4.1	2.3
NO_3^-(μg N L^{-1})	150	140	80
TSS (mg L^{-1})	n.d.	10.2	8.5
Chl-a (μg L^{-1})	24.5	18.8	20.2
Summer Bloom (max biomass fraction)	Dinophytes (99%)	Dinophytes (99%)	Cyanobacteria (85%)

Table 2. Ranges of gas concentrations over the entire water column (pelagial and littoral zones) and fluxes at the lake surface, as well as averaged masses (ranges in parentheses) of accumulated gases in Lake St. Augustin between June and October in 2010, 2011 and 2012.

Year	CO_2 Concentration / Flux (μM / mmol m^{-2} d^{-1})	CH_4 Concentration / Flux (μM / mmol m^{-2} d^{-1})	N_2O Concentration / Flux (nM / μmol m^{-2} d^{-1})	Mass CO_2 (10^5 mol)	Mass CH_4 (10^5 mol)	Mass N_2O (mol)
2010	3.4–125.2 / -33.7–18.9	0.11–2.1 / 0.09–3.8	1.1–1.9 / -0.2–1.3	0.64 ± 0.25 (0.33–1.02)	0.011 ± 0.006 (0.01–0.021)	3.4 ± 0.2 (3.0–3.7)
2011	6.0 – 93.5 / -22.7–61.0	0.03–1.5 / 0.08–2.3	0.65–17 / -1.9–37.8	0.63 ± 0.32 (0.18–1.1)	0.008 ± 0.004 (0.001–0.01)	4.2 ± 2.1 (1.9–7.2)
2012	4.7 – 65.0 / -30.1–82.9	0.05–5.2 / 0.15–7.5	0.5–9.8 / -1.62–8.7	0.34 ± 0.26 (0.16–1.32)	0.012 ± 0.006 (0.002–0.024)	5.3 ± 2.0 (2.3–9.8)

Table 3. Results of the stepwise multiple regression analysis relating GHGs accumulation to water temperatures (Ts-surface, ΔT – surface to bottom difference) and phytoplankton community structure in Lake Saint Augustin.

CO_2	Coef.	Std. Coef.	Std. Error	*p*
Constant	10.95		0.113	
Diatoms	0.06	0.45	0.0172	0.002

Dinophytes	-0.06	-0.36	0.022	0.01
ΔT	-0.14	-0.21	0.11	0.03
CH_4				
Constant	3.34		0.78	
Ts	1.17	0.61	0.26	0.001
Cyanobacteria	0.04	0.26	0.02	0.04
N_2O				
Constant	4.45		0.67	
Ts	-1.15	-0.84	0.25	0.001
ΔT	0.38	0.57	0.05	0.005

Table 4. Recent reports on processes controlling greenhouse gas fluxes in global lakes.

Process	Method	Main controlling factor	Affected gas (Pathway)	Reference
Eutrophication	Field survey	Chlorophyll-a	CH_4 (Diffusion)	Wang et al., 2006
	Incubations	Algal biomass	CH_4 (Diffusion)	Schwarz et al., 2008
	Incubations	Algal & terrestrial biomass	CH_4 (Total efflux)	West et al., 2012
	Field survey	Nutrients availability	CO_2 (Diffusion)	Pancheco et al., 2013
	Mesocosms	Chlorophyll-a	CH_4, CO_2 (Diffusion)	Davidson et al. 2015
	Field experiment	Food web structure	CH_4 (Diffusion)	Devlin et al., 2015
	Field survey	Chlorophyll-a	CH_4 (Total efflux)	West et al., 2015
	Modelling	Chlorophyll-a	CO_2, CH_4, N_2O (Total efflux)	DelSontro et al., 2018
	Incubations	Algal & terrestrial biomass	CH_4 (Total efflux)	Grasset et al., 2018
	Field survey	Dissolved organic matter	CH_4 (Diffusion)	Zhou et al., 2018
	Field survey	Nutrient availability	CO_2, CH_4, N_2O (Diffusion)	Klaus et al., 2018
	Meta-analysis	Chlorophyll-a	CH_4 (Total efflux)	Beaulieu et al., 2019

	Incubations	Nutrient availability/algal biomass	CH_4 (Total efflux)	Grasset et al., 2019
	Field survey	Nutrient availability/Chlorophyll-a	N_2O (Diffusion)	Webb et al., 2019
	Mesocosms	Chlorophyll/Dissolved organic matter	CH_4 (Ebullition)	Zhou et al., 2019
	Field survey	Nutrient availability	CH_4, N_2O (Diffusion)	Fernandez et al., 2020
	Mesocosms	Chlorophyll-a	CH_4, CO_2 (Total efflux)	Grasset et al., 2020
	Field survey	Chlorophyll-a	CH_4 (Diffusion)	Li et al., 2020
	Field survey	Nutrient availability/Chlorophyll-a	CH_4 (Diffusion)	Zhang et al., 2020
	Field survey	Nutrient availability	CH_4 (Diffusion)	Zhou et al., 2020
Climate change	Mesocosms	Warming	CO_2, CH_4 (Diffusion)	Durocher et al., 2011
	Field survey	Stratification strength	CO_2, CH_4 (Total efflux)	Zhu et al., 2018
	Mesocosms	Warming	CH_4 (Ebullition)	Davidson et al. 2018
	Field survey	Stratification strength	CH_4 (Total efflux)	Vachon et al., 2019
	Field experiment	Warming	N_2O (Diffusion)	Cheng et al., 2020
	Field survey	Stratification strength	CO_2 (Diffusion)	Pu et al., 2020
	Field survey	Stratification strength	CO_2, CH_4 (Total	Vachon et al.,

			efflux)	2020
Eutrophication & climate change	Field survey	Nutrient availability	CH_4 (Total efflux)	Gonzalez et al., 2014
	Field survey	Stratification/Hypoxia	CH_4, N_2O (Total efflux)	Salk et al., 2016
	Mesocosms	Nutrient availability/Chlorophyll-a	CO_2, CH_4, N_2O (Diffusion)	Audet et al., 2017
	Field survey	Chlorophyll-a/warming	CH_4 (Diffusion)	Xiao et al., 2017
	Mesocosms	Nutrient availability/warming	CH_4 (Diffusion)	Davidson et al., 2018
	Incubations	Nutrient availability/warming	CH_4 (Total efflux)	Sepulveda et al., 2018
	Field survey	Chlorophyll-a/warming	N_2O (Diffusion)	Xiao et al., 2018
	Field survey	Stratification/black bloom biomass	CH_4 (Diffusion)	Zhang et al., 2021
	Field survey	Warming/stratification/bloom and food web structure	CO_2, CH_4, N_2O (Total efflux)	Current study

Figures

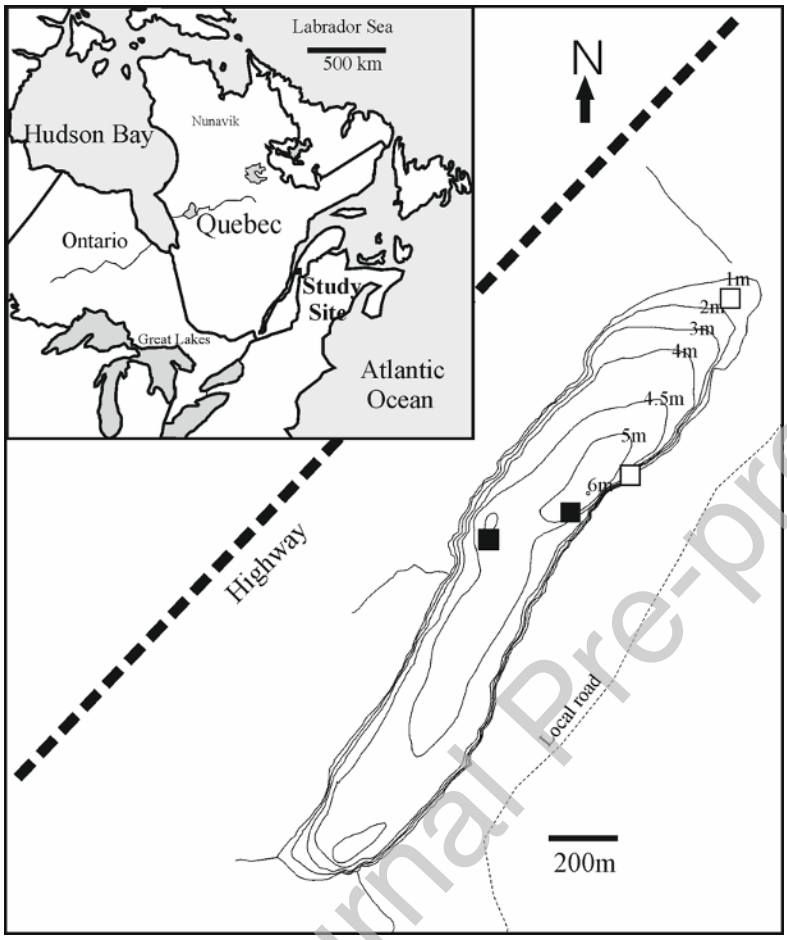

Figure 1. The bathymetry of Lake St. Augustin (Quebec, Canada) and location of sampling sites in the littoral and pelagial zones (white and black squares, respectively).

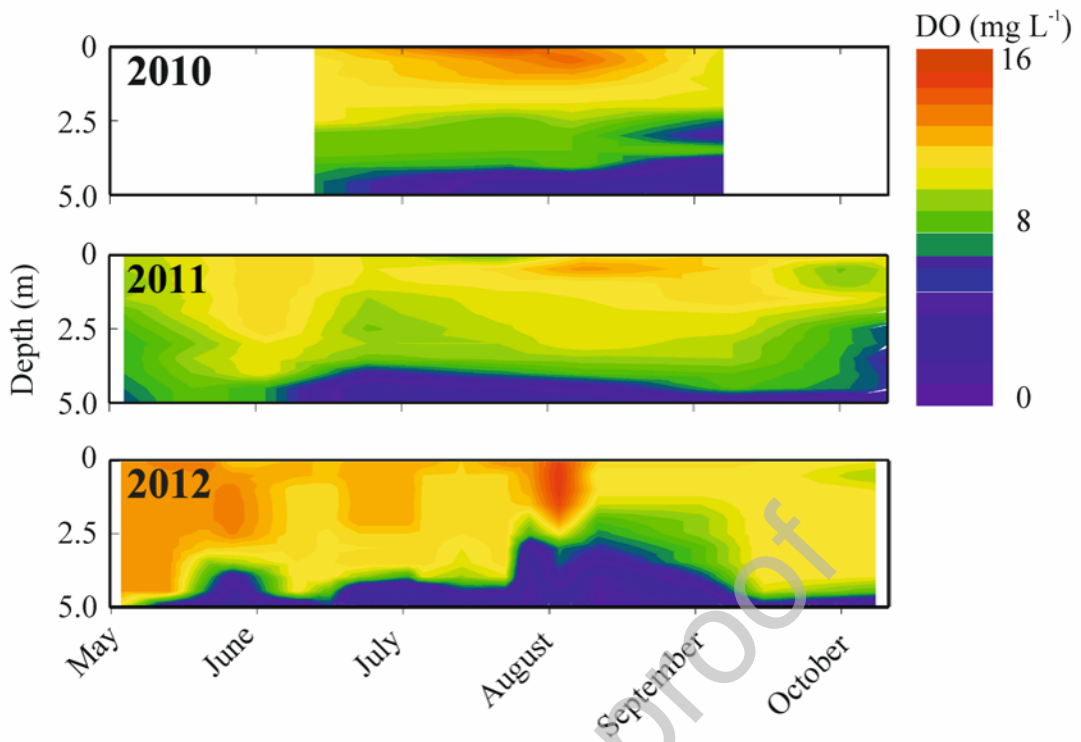

Figure 2. Oxygenation levels (interpolated from discrete water column profiles) in the water column of the pelagial zone of Lake St. Augustin during years with (2010 & 2012) and without heatwaves (2011). Heatwaves are defined as periods when air above the lake warmed beyond the pre-defined threshold of 31°C for at least 24h

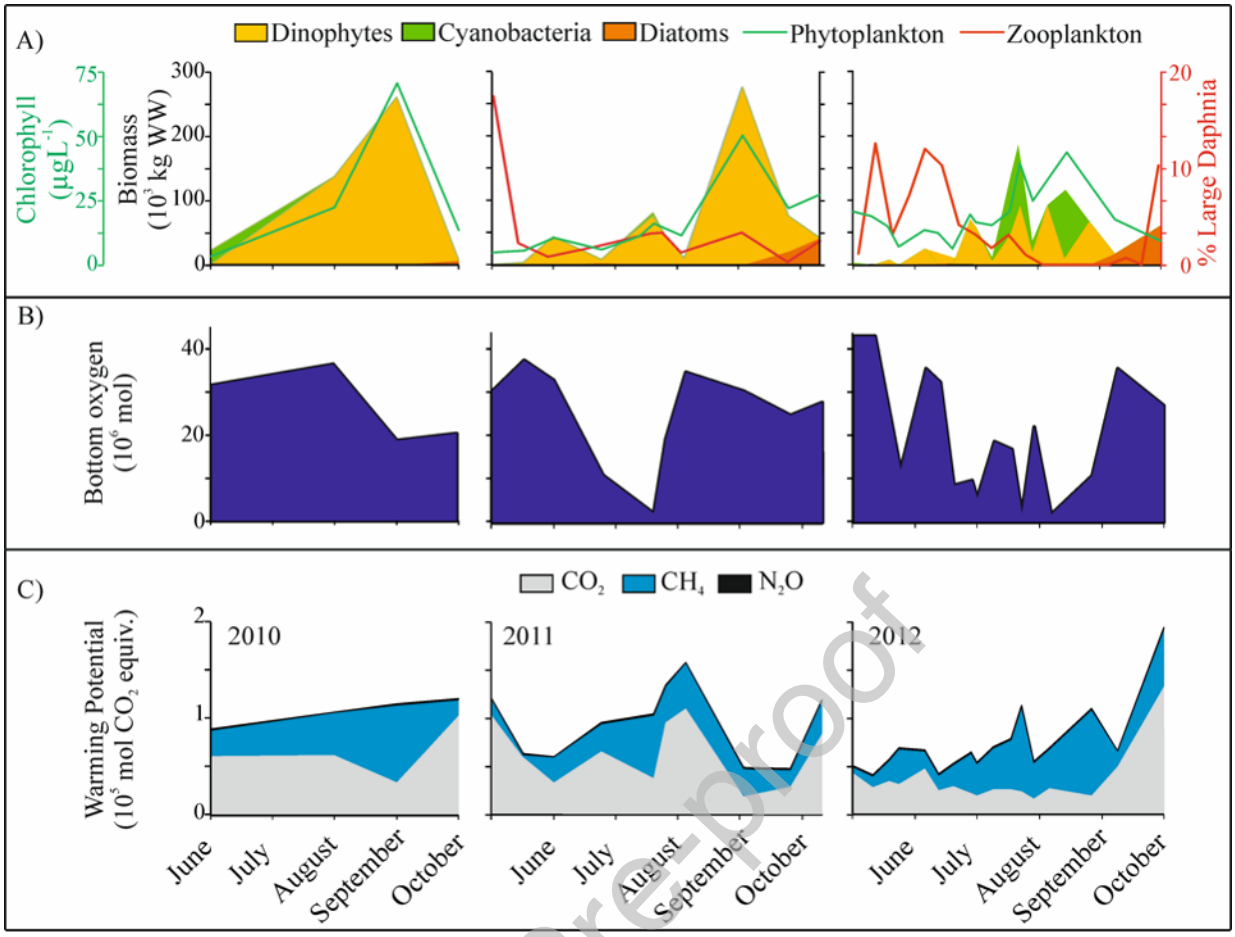

Figure 3. A) Total biomass (kg of wet weight) across total lake area of blooming phytoplankton (diatoms, cyanobacteria and dinophytes), average chlorophyll-a concentrations (in green) and relative abundance of large zooplankton (i.e., *Daphnia sp.;* in red) in the euphotic zone of Lake St. Augustin, B) Total amount of hypolimnetic oxygen (integrated between 4.5 and 6 m), and C) Inventory of stored greenhouse gases (CO_2, CH_4 and N_2O, given in CO_2 equivalents and integrated between 0 and 6 m) between June and October (2010-2012).

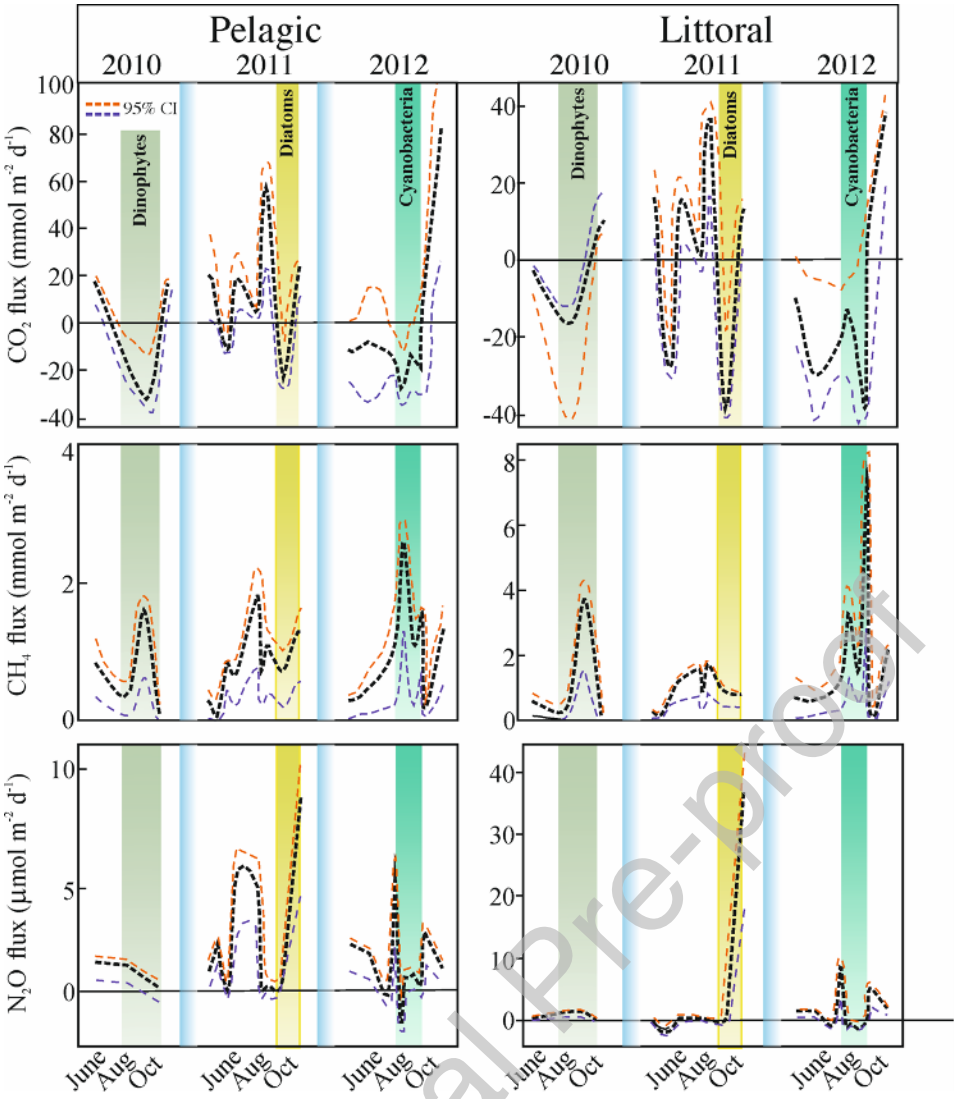

Figure 4. Diffusion of CO_2, CH_4 and N_2O (top to bottom panels) from the surface of Lake St. Augustin in the pelagial (left panels) and littoral zone (right panels) during the open-water season of the three studied years, showing different composition of phytoplankton blooms. Confidence intervals (95% CI) represent average gas fluxes ±2SD calculated using measurements of the departure from saturation for each GHG and two models estimating gas transfer velocities (Vachon & Prairie 2013; Cole and Caraco 1998).

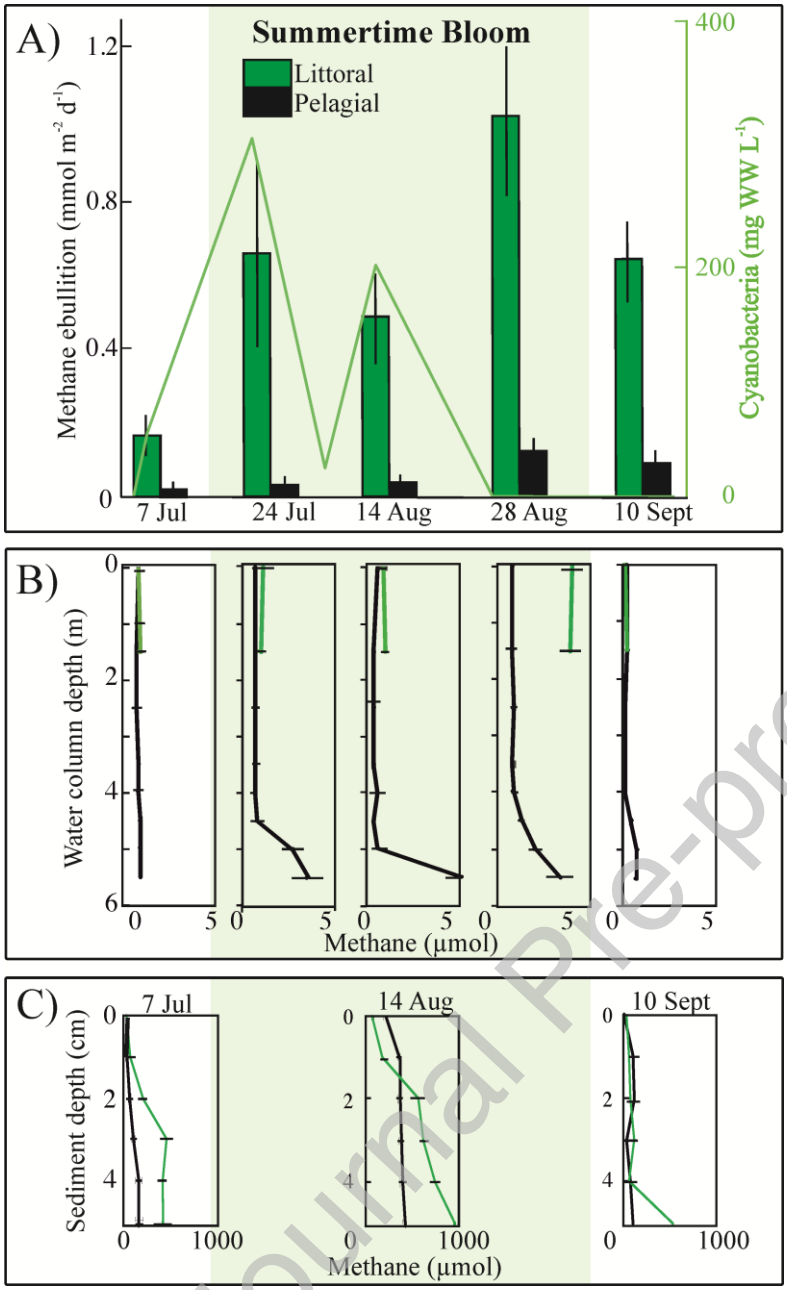

Figure 5. A) Methane ebullition rates (note: dates indicate timing of the initial funnel deployment, accumulated gas was collected between 3 to 4 days afterwards) and cyanobacteria biomass (in green); B) Distribution of CH_4 in the water column; C) Methane in the sediments of the littoral (in green) and pelagial (in black) zones before, during and after the cyanobacterial bloom in summer 2012 (sediments sampled at 1 cm and water column at 0.5 m resolution).

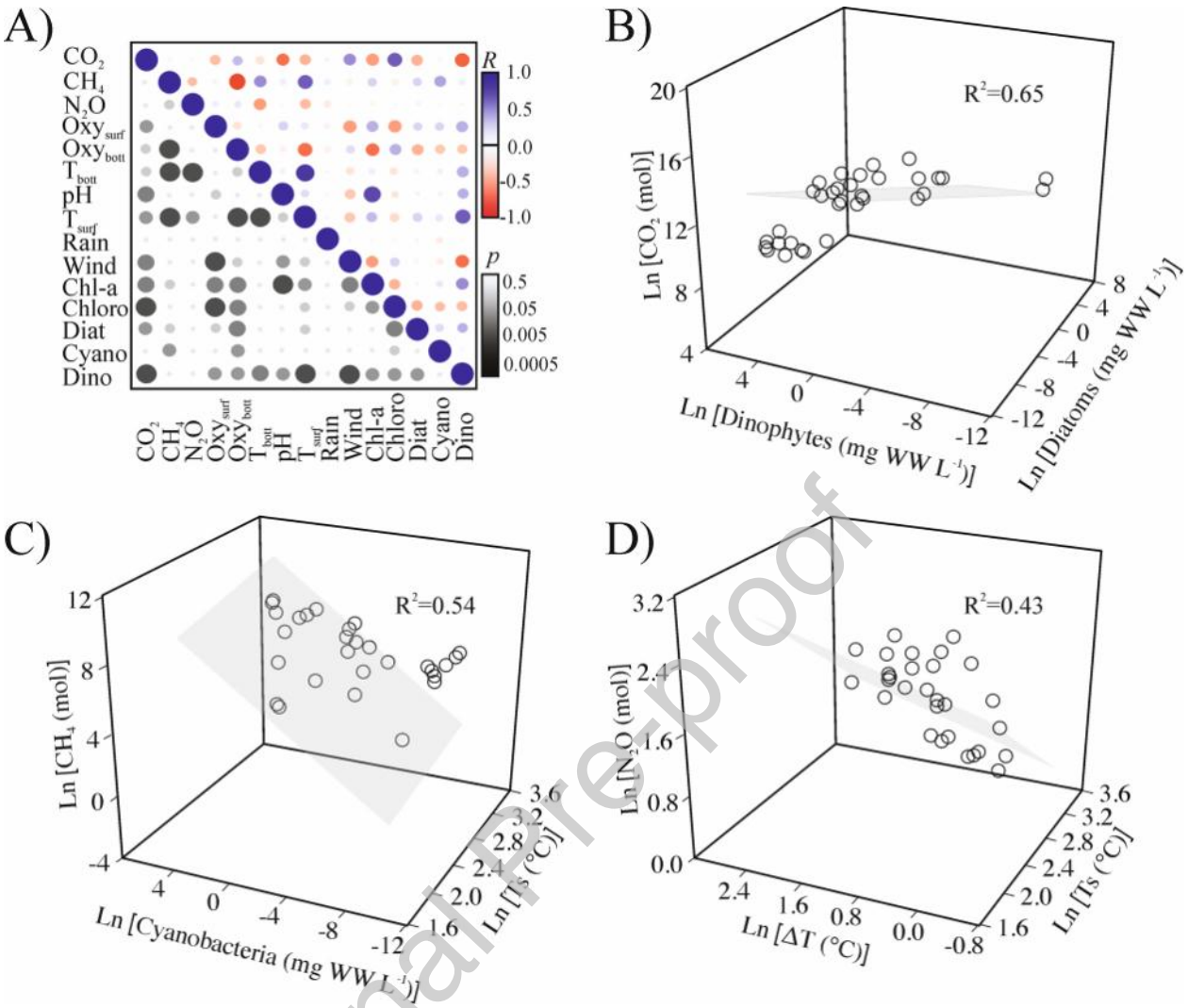

Figure 6. A) Pearson's correlation matrix (*R* and *p* values) between environmental conditions, phytoplankton community structure and different GHGs as well as results of the stepwise multiple regressions analysis between effects of water temperature, stratification and phytoplankton bloom biomass and community structure on GHGs stored in the water column of Lake St. Augustin during the studied periods in 2010-2012.